Sb−Sb Interactions in the Hafnium-Rich Antimonide Hf_6TiSb_4

Holger Kleinke[†]

FB Chemie und Wissenschaftliches Zentrum für Materialwissenschaften, Philipps-Universität Marburg, D-35032 Marburg, Germany

Received February 1, 1999

$(Hf,Ti)_7Sb_4$ is accessible via arc-melting of suitable mixtures of Hf, Ti, and $HfSb_2$. Its crystal structure is the first representative of a new structure type, as was determined by single-crystal analysis for $Hf_{7-x}Ti_xSb_4$ with $x = 1.05(7) \approx 1$. Hf_6TiSb_4 crystallizes in the monoclinic space group $P2_1/c$, with the lattice dimensions $a = 841.0(1)$, $b = 1102.9(1)$, $c = 1099.3(1)$ pm, and $\beta = 111.13(1)°$ ($Z = 4$). All seven independent metal sites are statistically occupied by different mixtures of hafnium and titanium, forming a three-dimensional network of metal atoms M which includes the Sb atoms in its (capped) square antiprismatic voids. The metal substructure can be described on the basis of semiregular 488 nets. Besides numerous M−Sb and M−M bonds, a nonlinear Sb_3 unit is present with bonding Sb−Sb interactions. Extended Hückel calculations, performed on the hypothetical model structure Hf_7Sb_4, point to metallic properties.

Introduction

Most metal-rich pnictides and chalcogenides exhibit M−M and M−pnicogen and M−chalcogen bonding, but no homonuclear bonds between the main group elements Q. A few exceptions including metals of the titanium group are uncovered, the structures of which consist in part of bonding Q−Q interactions, e.g., Ti_8Bi_9,[1] $Zr_2V_6Sb_9$,[2] ZrSb,[3] and $Zr_{7.5}V_{5.5}Sb_{10}$.[4] In these cases, the M/Q ratio is extended from 0.88 to 1.30. Considering the occurrence of Q−Q bonds as a hint to partially reduced species, it is not astonishing to find these bonds among the heavier pnictides rather than among the chalcogenides, because the latter are more electronegative on any electronegativity scale. On the other hand, it is likely that the more electropositive metal atoms reduce the Q atoms to a higher extent. From this point of view, the presence of Sb−Sb bonds in ZrSb was not expected, because TiSb,[5] NbSb,[6] and $V_{1+x}Sb$[7] all crystallize in the NiAs type without Sb−Sb contacts, while zirconium is more electropositive than titanium, niobium, and vanadium.

Here the new metal-rich antimonide Hf_6TiSb_4 is presented, which is by far the most metal metal-rich one being stabilized in part by Sb−Sb bonds. Furthermore, it consists mainly of hafnium atoms, which are even more electropositive than zirconium. Correspondingly, the Sb−Sb interactions are weaker, compared to the examples given above, but still present, as indicated by distances of the order of the second shortest Sb−Sb bond in elemental antimony. Comparisons with the binary hafnium pnictides of comparable metal/pnicogen ratio (e.g., Hf_5Sb_3[8] and Hf_7P_4[9]) will be discussed later in this article.

Experimental Section

Synthesis. $(Hf,Ti)_7Sb_4$ was prepared by arc-melting of $HfSb_2$, Hf, and Ti, corresponding to a ratio of Hf:Ti:Sb = 10:1:5 (Hf, STREM, powder, 99.6% (including up to 2.2% zirconium); Ti, ALFA, −100 mesh, 99.4%; Sb, MERCK, powder, 99.8%). $HfSb_2$ was chosen as the antimony source to minimize the loss of elemental antimony by vaporization during the process of arc-melting. It was synthesized by a reaction of the elements in the stoichiometric 1:2 ratio in an evacuated silica tube at 650 °C over a period of 5 days. The cold-pressed pellet of the starting materials was arc-melted twice after being inverted on a water-cooled copper block under a flow of argon of 3 L/min. Attempts to synthesize $(Hf,Ti)_7Sb_4$ by a solid-state reaction, i.e., by annealing of pressed pellets containing mixtures of Hf, $HfSb_2$, and Ti in sealed tantalum tubes at temperatures below 1250 °C, failed. On the other hand, the thermal stability of Hf_6TiSb_4 is rather high, because first, it was obtained directly from the melt, and, second, annealing of Hf_6TiSb_4 over a period of 7 days at 1000 °C in a Ta tube did not result in decomposition.

Phase Analysis. No known phases were detected by comparisons of the powder diffractogram of the arc-melted sample with the simulated histograms of possible binary antimonides, e.g., Hf_3Sb,[10] Hf_5Sb_3, Ti_3Sb,[11] and Ti_5Sb_3.[12] The conclusion that a ternary hafnium titanium antimonide formed was confirmed by subsequent investigations using an electron microscope (CAMSCAN, CS 4DV) with an additional EDX device (detector, NORAN INSTRUMENTS). No impurities were detected; the Hf:Ti:Sb ratio measured on selected crystals was roughly 6:1.1:4.1.

Structure Determination. A platelike single crystal was selected for the structure analysis using an IPDS diffractometer (STOE). The lattice parameters were calculated on the basis of the positions of 5000 reflections. The data were corrected for Lorentz and polarization effects. The systematic extinctions ($l = 2n + 1$ for all $h0l$ reflections, and $k = 2n + 1$ for all $0k0$) are in agreement with the centrosymmetric space group $P2_1/c$, which was chosen for the structure solution and refinement

[†] E-mail: kleinke@mailer.uni-marburg.de.

(1) Richter, C. G.; Jeitschko, W. *J. Solid State Chem.* **1997**, *134*, 26.
(2) Kleinke, H. *Eur. J. Inorg. Chem.* **1998**, 1369.
(3) Garcia, E.; Corbett, J. D. *J. Solid State Chem.* **1988**, *73*, 452.
(4) Kleinke, H. *J. Chem. Soc., Chem. Commun.* **1998**, 2219.
(5) Nowotny, H.; Peal, J. *Monatsh. Chem.* **1951**, *82*, 336.
(6) Myzenkova, L. F.; Baron, V. V.; Savitsky, Y. M. *Russ. Metall.*, transl. from *Izv. Akad. Nauk SSR, Met.* **1966**, 89.
(7) Bouwma, J.; van Bruggen, C. F.; Haas, C. *J. Solid State Chem.* **1973**, *7*, 255.
(8) Kleinke, H.; Felser, C. *J. Alloys Compd.* Submitted for publication.
(9) Kleinke, H.; Franzen, H. F. *Angew. Chem., Int. Ed. Engl.* **1996**, *35*, 1934.
(10) Schubert, K.; Raman, A.; Rossteutscher, W. *Naturwissenschaften* **1964**, *51*, 506.
(11) Ramakrishnan, S.; Chandra, G. *Phys. Lett.* **1984**, *100A*, 441.
(12) Berger, R. *Acta Chem. Scand.* **1977**, *31A*, 889.

10.1021/ic990138m CCC: $18.00 © 1999 American Chemical Society
Published on Web 05/22/1999

Table 1. Crystallographic Data for $Hf_{5.95(7)}Ti_{1.05}Sb_4$

chemical formula: $Hf_{5.95(7)}Ti_{1.05}Sb_4$	formula weight: 1599.31 g/mol
$a = 841.0(1)$ pm	space group: $P2_1/c$ (no. 14)
$b = 1102.9(1)$ pm	$T = 22$ °C
$c = 1099.3(1)$ pm	$\lambda = 71.069$ pm
$\beta = 111.13(1)°$	$\rho_{calcd} = 11.17$ g/cm^3
$V = 951.1(2) \times 10^6$ pm^3	$\mu = 765.2$ cm^{-1}
$Z = 4$	$R(F_o)^a = 0.038$; $R_w(F_o^2)^b = 0.071$

$^a R(F_o) = \sum||F_o| - |F_c||/\sum|F_o|$. $^b R_w(F_o^2) = [\sum[w(F_o^2 - F_c^2)^2]/\sum[w(F_o^2)^2]]^{1/2}$.

Table 2. Positional Parameters, Equivalent Displacement Parameters, and Occupancy Factors (M = Hf, Ti)

site	x	y	z	U_{eq}/(10^4 pm^2)	occupancy
M1	0.1983(2)	0.0005(1)	0.5541(2)	0.0110(5)	0.889(9)Hf + 0.111Ti
M2	0.4022(2)	0.0534(1)	0.3461(1)	0.0096(5)	0.87(1)Hf + 0.13Ti
M3	0.6298(2)	0.05355(9)	0.1398(1)	0.0102(5)	0.89(1)Hf + 0.11Ti
M4	0.9899(2)	0.2039(1)	0.0619(2)	0.0114(5)	0.84(1)Hf + 0.16Ti
M5	0.9910(2)	0.07341(9)	0.7913(1)	0.0088(5)	0.832(9)Hf + 0.168Ti
M6	0.6427(2)	0.22743(9)	0.8286(1)	0.0092(5)	0.83(1)Hf + 0.17Ti
M7	0.3457(2)	0.2407(1)	0.0210(1)	0.0086(5)	0.804(9)Hf + 0.196Ti
Sb1	0.9951(3)	0.1593(1)	0.3322(2)	0.0093(5)	1Sb
Sb2	0.2370(3)	0.0063(1)	0.0641(2)	0.0112(5)	1Sb
Sb3	0.2816(3)	0.1906(1)	0.7540(2)	0.0129(5)	1Sb
Sb4	0.6923(3)	0.1840(1)	0.5855(2)	0.0142(5)	1Sb

(SHELXS/SHELXL[13]). The structure solution yielded 11 atom sites on general positions. Seven Hf and four Sb atoms were tentatively assigned on the basis of the heights of the peaks and the interatomic distances. While no residual peaks suitable for Ti atoms occurred in the difference Fourier map of the following structure refinement, the equivalent displacement parameters of the Hf atoms were more than twice as large as the corresponding parameters of the Sb atoms, indicating different mixed Hf/Ti occupancies. All metal sites M1−7 were then refined as being mixed occupied by Ti and Hf, which resulted in significantly enhanced residual values (e.g., a decrease in $R(F)$ from 0.043 to 0.038) and reasonable displacement parameters between $U_{eq} = 0.0086(5) \times 10^4$ and $0.0114(5) \times 10^4$ pm^2, which are comparable to the U_{eq}'s of the Sb sites (ranging from $0.0097(5) \times 10^4$ to $0.0142(5) \times 10^4$ pm^2). Further crystallographic details are given in Table 1. Positional parameters, occupancy factors, and equivalent displacement parameters are listed in Table 2. Interatomic distances may be found in Table 3.

Calculations. Extended Hückel calculations[14−16] were carried out on the hypothetical model structure Hf_7Sb_4 using a mesh of 128 k points; i.e., the structure experimentally determined for $(Hf,Ti)_7Sb_4$ was taken with hafnium parameters for all metal sites, since mixed occupancies cannot be handled within the theory. The ionization potentials were optimized by charge iteration in Hf_5Sb_3. All parameters used are listed in Table 4.

Results and Discussion

Crystal Structure. $(Hf,Ti)_7Sb_4$ is a typically DFSO-stabilized material like $(Hf,Ti)_{21}S_8$;[17] i.e., *d*ifferential *f*ractional site *o*ccupancies enhance significantly the stability of the compound. This concept was developed by Franzen et al.[18,19] after the successful characterization of four ternary niobium tantalum sulfides, $Nb_{1.72}Ta_{3.28}S_2$,[20] $Nb_{1.90}Ta_{2.10}S_2$,[21] $Nb_{4.92}Ta_{6.08}S_4$,[22] and $Nb_{6.74}Ta_{5.26}S_4$,[23] whose structures are unknown among the binary niobium sulfides as well as among the tantalum sulfides. Franzen et al. postulated three criteria for ternary DFSO-stabilized materials as follows: (i) each metal atom site is mixed occupied without long-range order by two different metal atoms, (ii) the fractional site occupancies, being more or less fixed per site, differ from one site to another, and (iii) the crystal structures are not found in the binary systems. This concept was subsequently expanded to include metals of different groups (e.g., Zr/Nb in $Zr_{6.45}Nb_{4.55}P_4$[24]) and quaternary compounds ($Hf_{10-x}Nb_xNi_3P_5$[25]).

Table 3. Selected Interatomic Distances [pm] (M−M < 400, M−Sb < 350, Sb−Sb < 400 pm, M = Hf, Ti)

M1−Sb4	289.1(5)	M2−Sb4	291.3(3)	M3−Sb2	292.0(9)
M1−Sb3	293.4(5)	M2−Sb2	295(1)	M3−Sb3	292.3(3)
M1−Sb1	296.3(7)	M2−Sb3	304.7(4)	M3−Sb4	303.9(2)
M1−Sb1	299(1)	M2−M7	312.1(3)	M3−M7	307.0(1)
M1−M1	311(1)	M2−M1	319(1)	M3−Sb2	314.6(9)
M1−M7	318.5(2)	M2−M6	320.1(2)	M3−M6	316.1(2)
M1−M2	319(1)	M2−Sb4	321(2)	M3−M1	320(1)
M1−M3	320(1)	M2−M1	337(1)	M3−Sb1	325(2)
M1−M6	335.8(5)	M2−M2	340(2)	M3−M3	328(2)
M1−M2	337(1)	M2−M5	340(1)	M3−M5	331.1(7)
M1−M5	364(2)	M2−M3	345(1)	M3−M2	345(1)
M1−M4	365.7(5)	M2−Sb1	356.8(3)	M3−M7	373.6(2)
M1−M5	371(1)	M2−M6	359.2(3)	M3−M4	381.1(7)
M1−M4	371.8(2)			M3−M6	394.3(3)
				M3−M6	395.7(2)
M4−Sb3	285(2)	M5−Sb3	292.1(4)	M6−Sb2	286.3(4)
M4−Sb4	288.6(4)	M5−Sb1	292.5(2)	M6−Sb4	287.3(5)
M4−Sb1	295.6(3)	M5−Sb4	297(2)	M6−Sb3	287.5(9)
M4−Sb1	299.6(3)	M5−Sb1	298.0(2)	M6−Sb4	289.0(5)
M4−Sb2	300.4(8)	M5−Sb2	302.9(1)	M6−M4	313(2)
M4−Sb2	300.5(3)	M5−Sb2	306(2)	M6−M3	316.1(2)
M4−M6	313(2)	M5−M4	330.8(2)	M6−M2	320.1(2)
M4−M7	320.8(5)	M5−M3	331.1(7)	M6−Sb1	320.3(3)
M4−M5	330.8(2)	M5−M2	340(1)	M6−M1	335.8(5)
M4−M5	343.4(2)	M5−M4	343.4(2)	M6−M7	342(2)
M4−M5	351.8(2)	M5−M4	351.8(2)	M6−M5	353.6(4)
M4−M1	365.7(5)	M5−M6	353.6(4)	M6−M2	359.2(3)
M4−M1	371.8(2)	M5−M7	364(2)	M6−M7	381(1)
M4−M3	381.1(7)	M5−M1	364(2)	M6−M3	394.3(3)
		M5−M1	371(1)	M6−M3	395.7(2)
M7−Sb2	283.8(3)	Sb1−Sb3	328.3(7)	Sb2−Sb2	372(1)
M7−Sb3	284.1(6)	Sb1−Sb4	344(2)	Sb2−Sb3	388.7(3)
M7−Sb4	286.3(7)				
M7−Sb3	290.2(5)	Sb3−Sb1	328.3(7)	Sb4−Sb1	344(2)
M7−M3	307.0(1)	Sb3−Sb2	388.7(3)		
M7−M2	312.1(3)				
M7−Sb1	313(2)				
M7−M1	318.5(2)				
M7−M4	320.8(5)				
M7−M6	342(2)				
M7−M5	364(2)				
M7−M3	373.6(2)				
M7−M6	381(1)				

Table 4. Parameters Used for Extended Hückel Calculations on Hypothetical Hf_7Sb_4

orbital	H_{ii}/eV	ζ_1	c_1	ζ_2	c_2
Hf, 6s	−8.26	2.21			
Hf, 6p	−4.69	2.17			
Hf, 5d	−8.25	4.36	0.6967	1.709	0.5322
Sb, 5s	−18.80	2.32			
Sb, 5p	−11.70	2.00			

(13) Sheldrick, G. M. *SHELXS-86/SHELXL-97*; Universität Göttingen: Germany, 1986−1997.
(14) Hoffmann, R. *J. Chem. Phys.* **1963**, *39*, 1397.
(15) Whangbo, M.-H.; Hoffmann, R. *J. Am. Chem. Soc.* **1978**, *100*, 6093.
(16) Program EHMACC, adapted for use on a PC by M. Köckerling, Gesamthochschule Duisburg, 1997.
(17) Harbrecht, B.; Franzen, H. F. *Z. Kristallogr.* **1989**, *186*, 119.
(18) Yao, X.; Marking, G. A.; Franzen, H. F. *Ber. Bunsen-Ges. Phys. Chem.* **1992**, *96*, 1552.
(19) Franzen, H. F.; Köckerling, M. *Prog. Solid State Chem.* **1995**, *23*, 265.
(20) Yao, X.; Franzen, H. F. *J. Am. Chem. Soc.* **1991**, *113*, 1426.
(21) Yao, X.;. Miller, G. J.; Franzen, H. F. *J. Alloys Compd.* **1992**, *183*, 7.
(22) Yao, X.; Franzen, H. F. *J. Solid State Chem.* **1990**, *86*, 88.
(23) Yao, X.; Franzen, H. F. *Z. Anorg. Allg. Chem.* **1991**, *589/599*, 353.
(24) Marking, G. A.; Franzen, H. F. *Chem. Mater.* **1993**, *5*, 678.
(25) Kleinke, H.; Franzen, H. F. *J. Am. Chem. Soc.* **1997**, *119*, 12824.

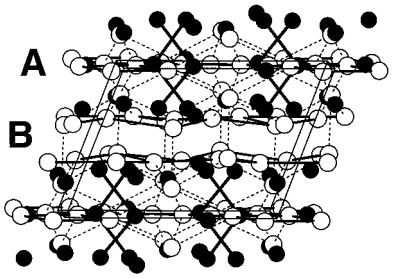

Figure 1. Projection of the structure of $(Hf,Ti)_7Sb_4$ along [010]. Horizontal, *c* axis. White circles, M; black, Sb. Thin lines, M−M distances within the *b*,*c* plane; dashed, M−M connecting the units **A** and **B**; thick, Sb−Sb < 350 pm.

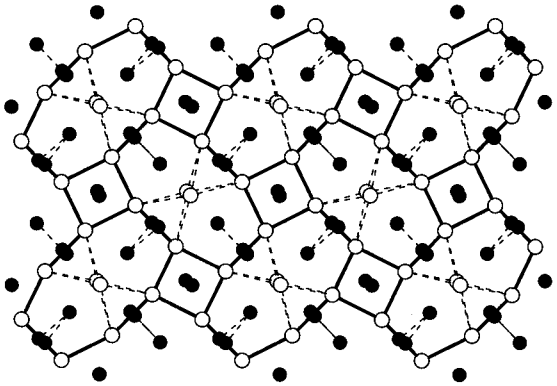

Figure 2. Projection of the M layer **A** onto the *b*,*c* plane, including the Sb1 atoms, sheathed by M1 and Sb2 atoms. Horizontal, *b* axis. White circles, M; black, Sb. Thick lines emphasize the 488 tiling. Dashed lines, Sb−Sb < 350 pm and M−M distances including M1.

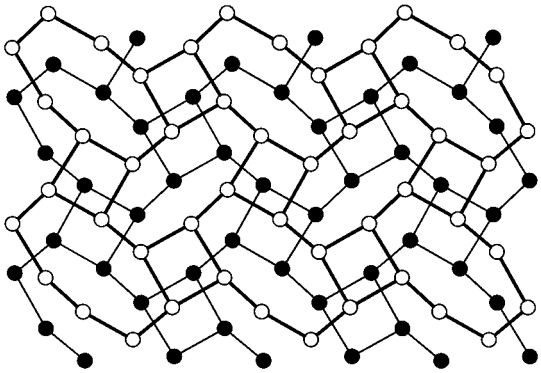

Figure 3. Projection of the M double layer **B** onto the *b*,*c* plane. Horizontal, *b* axis. The lines emphasize the 488 tiling. The different heights are reflected in different shadings.

No other binary antimonide, including Hf and Ti antimonides, with a metal/antimony ratio of 7:4 has been found to date. It is concluded that the mixed occupancies observed here favor the formation of this new structure type. The rather complex crystal structure of $(Hf,Ti)_7Sb_4$ is shown in a slightly tilted projection along the crystallographic *b* axis in Figure 1. While M−M bonds are extended to form a three-dimensional metal substructure, one can formally divide the structure into three sections parallel to the *b*,*c* plane. At $x \approx 0$, an almost planar layer (**A**) is formed by the M4,5 and Sb1 atoms, as depicted in Figure 2. A nonlinear Sb_3 unit (thick lines in Figure 1) is located perpendicular to **A**. A metal double layer (**B**) is located around $x = {}^1/_2$, consisting of the metal sites M2,3,6,7 (Figure 3). The area between **A** and **B** is predominated by Sb atoms, but includes also the M1 atoms. M−M, M−Sb, and Sb−Sb interactions connect all sections to a truly three-dimensional structure.

For better understanding, the two layers **A** and **B** will be discussed in some detail. The two M atoms M4 and M5 form an almost perfectly planar square in layer **A**, with M−M contacts of 331 and 343 pm and bond angles of 89 and 91°, respectively. The squares, being capped by two Sb2 atoms to form M_4Sb_2 octahedra, are interconnected via a longer M4−M5 distance of 352 pm in such a way that a semiregular 488 tiling is formed. Each elongated octagon includes two Sb1 atoms, while its center is capped by two M1 atoms. The Sb1 atoms are located within the same plane, forming four Sb−M bonds to two different squares. The shortest distance between the M1 atoms and the M atoms of **A** of 364 pm is significantly longer than the distance between the M1 atoms of 311 pm. However, each M1 atom forms four bonds to the Sb1 atoms < 300 pm.

The double layer **B** consists of two semiregular 488 nets, also, which are related by symmetry (e.g., an inversion center between the layers). Thus, **B** contains two quasiplanar layers which correspond topologically to the metal substructure of **A**. While the M−M bonds of the squares in **A** are shorter than between the squares (331/343 versus 352 pm), the opposite is true in **B**: the shortest distances (312 and 316 pm) connect the squares, in which longer distances occur (359, 374, 396, and 400 pm). As a result, the octagons are more elongated in **B**, compared to **A**. Furthermore, the "squares" are more irregular. Short M−M distances between 307 and 328 pm connect the two 488 nets of B, while the M1 atoms cap the octagons of **B** on one side as in **A**. The three-dimensionality of the M substructure is the result of the M1 atoms forming M−M bonds to **A** as well as to **B**. The similarities between the units **A** and **B** are completed by the Sb2 atoms, which are located between the squares of **A** and **B**. Additionally, the Sb4 atoms are situated within the octagons of **B** (slightly shifted out of the plane) as the Sb1 atoms in **A**.

For comparisons of the M−M distances with other metal-rich compounds, it should be noted that the occupancies of the M sites vary from 89% Hf and 11% Ti to 80% Hf and 20% Ti. Thus, the most reasonable comparisons are those with Hf-rich antimonides, namely Hf_5Sb_3[8] and Hf_6NiSb_2:[26] in all cases, the shortest Hf−Hf distances are comparable to the short Hf−Hf bonds in the hexagonal modification of elemental hafnium (313 and 320 pm). For example, in the structure of Hf_5Sb_3 (Y_5Bi_3 type), Hf−Hf bond lengths from 307 to 318 pm occur, while the shortest ones in the structure of Hf_6NiSb_2 vary between 321 and 329 pm.

The M−Sb bonds are extended over a fairly large range from 284 to 325 pm, comparable to the situation observed for the Hf−Sb bonds in Hf_5Sb_3 (280−318 pm), while the Ti−Sb bonds in Ti_5Sb_3 range from 271 to 295 pm. On average, Ti−Sb bonds are shorter than Hf−Sb bonds because of the smaller radius of a Ti atom, compared to Hf (Pauling single bond radii: r_{Ti} = 132 pm; r_{Hf} = 144 pm[27]). This size difference is reflected in the averaged M−Sb distances, which are smallest for the M site with the smallest Hf content (M7: 80% Hf). The correlation between Hf occupancies and averaged M−Sb distances is not very strong, as Figure 4 reveals, because other factors also play a role for the site preferences of hafnium, e.g. the higher cohesive energy and the lower electronegativity, compared to titanium. This will be discussed under Electronic Structure below.

Since the M−Sb distances depend on the coordination numbers (CN), the different numbers of neighboring Sb atoms

(26) Kleinke, H. *J. Alloys Compd.* **1998**, *270*, 136.
(27) Pauling, L. *The Nature of the Chemical Bond*, 3rd ed.; Cornell University Press: Ithaca, NY, 1948.

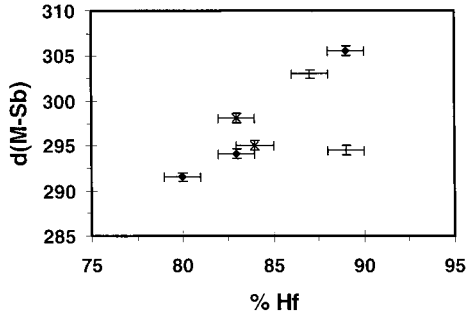

Figure 4. Hf occupancy per M site versus averaged M−Sb distances [pm]. +, CN = 4; ◆, CN = 5; ×, CN = 6.

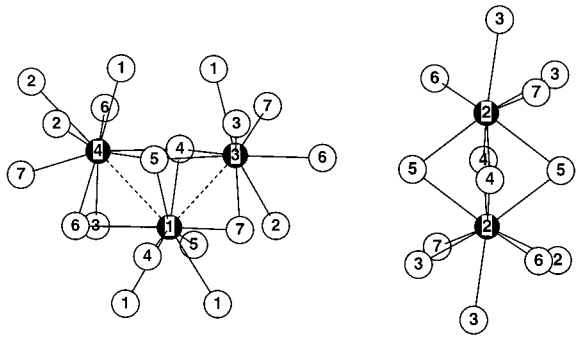

Figure 5. Coordination spheres of the Sb atoms. White circles, M; black, Sb.

are reflected in different symbols in Figure 4. No trend can be depicted for the M sites with four (marked with +) and six (×) Sb neighbors, because their occupancies differ only within the standard deviations. On the other hand, in the case of the three sites with five Sb neighbors (◆), the Hf content clearly increases with increasing M−Sb distances.

The two different Sb units in $(Hf,Ti)_7Sb_4$ (a Sb_3 unit, consisting of Sb1,3,4, and a Sb atom (Sb2) without neighboring Sb atoms) are shown in Figure 5. All Sb atoms are situated in (somewhat distorted) square antiprisms formed by eight M atoms, which are capped by a ninth M atom in the cases of Sb1,2,4. The polyhedra are more or less irregular, so that they could also be regarded as bi- and tricapped trigonal prisms to a first approximation. Then, the relations between $(Hf,Ti)_7Sb_4$ and the binaries Hf_7P_49 and Hf_5Sb_3 become more clear, because the coordination spheres of the pnicogen atoms (Q = P, Sb) of the binaries are described best as mono-, bi-, and tricapped trigonal prisms, respectively. In only the structure of $(Hf,Ti)_7Sb_4$, additional Q atoms complete the coordination spheres, namely two in the case of Sb1 and one in the cases of Sb3 and Sb4. The averaged coordination numbers of the Q atoms increase with decreasing r_M/r_Q ratio from 8.25 in Hf_7P_4 over 9.0 in Hf_5Sb_3 to 9.75 in $(Hf,Ti)_7Sb_4$ (with $r_P = 110$ and $r_{Sb} = 139$ pm,[27] the r_M/r_Q ratios are 1.31, 1.04, and 1.02, respectively). The difference in the M/Sb ratio between Hf_5Sb_3 (M/Sb = 1.6) and $(Hf,Ti)_7Sb_4$ (M/Sb = 1.75) is also a reason for the higher coordination number of the Sb atoms in $(Hf,Ti)_7Sb_4$. The high coordination numbers of the Sb sites in the structure of $(Hf,Ti)_7Sb_4$ implies that $(Hf,Ti)_7Sb_4$ does not form a structure with a *bcc* metal substructure with Sb atoms in its capped prismatic voids because of the maximal coordination number of the interstitials of 9 in that kind of structures.

The Sb2−Sb2 distance of 372 pm is too long to enable significant contact, whereas the two Sb−Sb contacts of 328 and 344 pm within the Sb_3 unit shown in Figure 5 are comparable to the Sb−Sb distance between Sb atoms of neighbored layers in elemental antimony (336 pm), where bonding character can be assumed based on the truly three-dimensional mechanical and physical properties. Based on the comparable lengths, weak bonding character is postulated in this case, also. As depicted with thick lines in Figure 1, these contacts occur within a nonlinear Sb3−Sb1−Sb4 unit (bond angle 87°), which crosses the layer **A**. To date, comparable bond lengths in transition metal antimonides were restricted to compounds with a M/Sb ratio < 1.5, e.g., $Zr_{7.5}V_{5.5}Sb_{10}$, V_3Sb_2,[28] ZrSb, and $Zr_2V_6Sb_9$. In the structures of these examples, the bonding Sb−Sb interactions range from 280 to 343 pm, with the majority at distances around 330 pm. Compounds with higher M/Sb ratios usually show a complete reduction of Sb to Sb^{3-} and thus well separated Sb sites. Furthermore, since vanadium is here the most electronegative metal atom, the occurrence of Sb−Sb bonds of ca. 320 pm and thus relatively poorly reduced Sb atoms in V_3Sb_2 is less surprising than finding Sb−Sb bonds in Hf_6TiSb_4, a compound with a more electropositive metal (hafnium) as major component and a higher M/Sb ratio. A comparison with the less metal-rich binary titanium and hafnium antimonides Ti_5Sb_3 and Hf_5Sb_3, whose structures exhibit no Sb−Sb bonding, points to heteroatomic interactions being favored already at M/Sb = 1.6. It is concluded that the structure of $(Hf,Ti)_7Sb_4$ is additionally stabilized by a gain in the configurational entropy due to mixed site occupancies.

Electronic Structure. The calculations were performed in order to gain information about the physical properties as well as the bonding situation. Calculations of the model structure Hf_7Sb_4 are most likely sufficient for drawing qualitative conclusions, because first, the Ti content varies only from 9 to 20% from site to site, and second, titanium and hafnium are isovalent. The densities of states (DOS) and selected crystal orbital overlap populations are shown in Figure 6. Within the energy window shown, the DOS consists of two parts: the peak at lower energies between −15 and −10.5 eV has mainly Sb *p* character (with the *s* states of Sb located below the energy window of −16 to −6 eV), while some Hf contributions to this peak point to a covalent character of the Hf−Sb interactions. The second part, the conduction band, is predominated by the d states of hafnium, but contains some contributions of antimony, also, well separated from the lower peak by a small band gap < 0.5 eV. Although the Fermi level is situated close to a local minimum in the conduction band, a significant number of states remain at its energy level of −8.57 eV. This situation, combined with the occurrence of M−M contacts along all axes of the unit cell of $(Hf,Ti)_7Sb_4$, occurs by all indications with metallic properties.

The crystal orital overlap population (COOP) curves of the Hf−Hf and Hf−Sb interactions are comparable to those of Hf_5Sb_3. In both cases, almost no antibonding states occur below the Fermi level, and additional valence electrons would fill more Hf−Hf bonding, but Hf−Sb antibonding states, also. Both different kinds of interactions are substantial contributions to the stability of $(Hf,Ti)_7Sb_4$.

Although hafnium and titanium are in different periods of the periodic table of elements, no strong correlation was found between the different site occupancies and the Hf−Hf or Hf−Sb interactions. Some basic trends more or less equalize each other: the larger extension of the 5d orbitals of hafnium, compared to the 3d orbitals of titanium (a fact which is reflected in the higher cohesive energy of hafnium (619(4) versus 470(2) kJ/mol[29]), and the higher electropositive character enables hafnium to form stronger metal−metal as well as metal−

(28) Steinmetz, J.; Malaman, B.; Roques, B. *Compt. Rend.* **1977**, *284C*, 499.

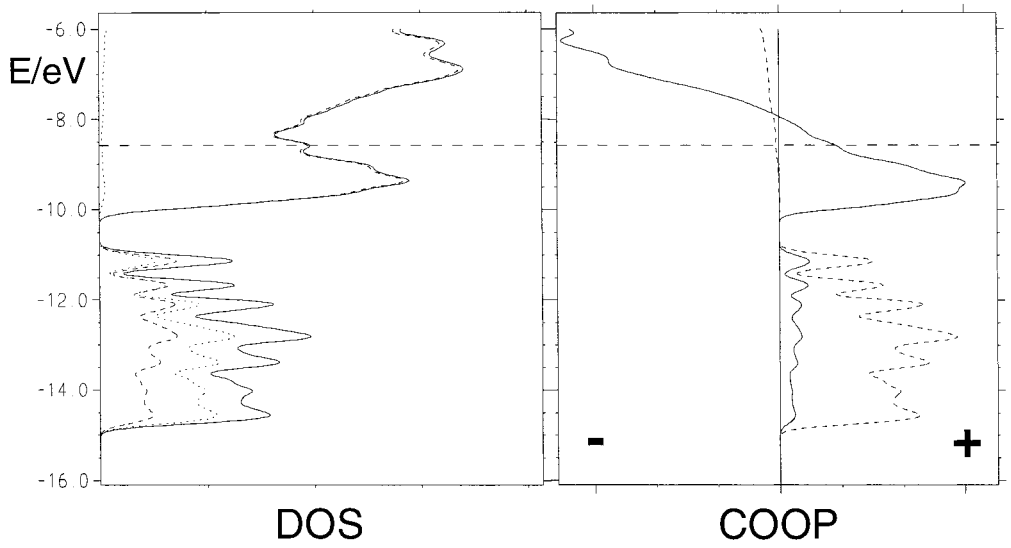

Figure 6. Left: densities of states (DOS) of the structure model Hf_7Sb_4. Dashed horizontal line, Fermi level. Solid line, total DOS; dashed, Hf; dotted, Sb contributions. Right: crystal orbital overlap populations (COOP). Solid line, Hf−Hf; dashed, Hf−Sb interactions, summed over all bonds of the unit cell. Right part of the diagram, bonding (+); left, antibonding (−) interactions.

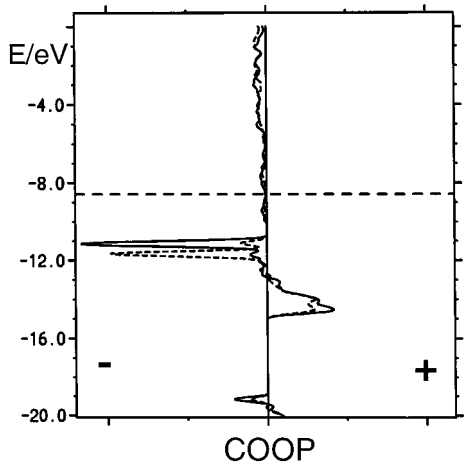

Figure 7. Crystal orbital overlap populations (COOP). Solid line, Sb1−Sb3 (328 pm); dashed, Sb1−Sb (344 pm) bond. Right part of the diagram, bonding (+); left, antibonding (−) interactions.

antimony bonds, which leads to hafnium preferring the sites with the higher M−M and M−Sb overlap populations. Furthermore, the M−M overlap populations generally increase with decreasing interatomic distances, and Ti prefers the smaller bonds because of its smaller size, compared to Hf. These opposite preferences impeded the occurrence of clear trends in the structure of the sulfide $(Hf,Ti)_{21}S_8$, also.

The COOP curves of the two shortest Sb−Sb interactions of 328 and 344 pm, averaged per bond, are depicted in Figure 7. In both cases, antibonding states predominate above −13 eV, i.e., well below the Fermi level, which is a consequence of the almost filled p states of the participating Sb atoms, the most electronegative kind of atoms in this structure.

The presence of unoccupied states well above the Fermi level strongly suggests that these Sb atoms are not completely reduced. Net small, but positive overlap populations are calculated as the result of the sums of filled bonding and antibonding states for both interactions, namely 0.053 electron per bond for the shorter and 0.023 for the longer one. Similar values were obtained for the bonds between 336 and 343 pm in $Zr_2V_6Sb_9$ (from 0.048 to 0.025) and for the longer bond of 336 pm in elemental antimony (0.077), using the same Hückel parameters for the Sb atoms.[2] Marginal differences in the Mulliken charges show that Sb atoms with stronger or more Sb−Sb interactions are less reduced: these charges increase by going from Sb1 (charge −0.32, two Sb−Sb bonds) to Sb4 (−0.34, one bond, the weaker one) and Sb3 (−0.35, one bond, the stronger one) to Sb2 (−0.42, no Sb−Sb distance < 370 pm), while the same trend was observed in the case of $Zr_2V_6Sb_9$; i.e., the most reduced Sb atom takes part in the fewest and/or weakest Sb−Sb bonds.

Summary

The new metal-rich antimonide $Hf_{5.95(7)}Ti_{1.05}Sb_4$ has been synthesized and characterized with respect to its crystal as well as its electronic structure. In this new structure type, a three-dimensional network of M atoms, consisting in part of semi-regular 488 nets, surrounds the Sb atoms in square antiprismatic voids. The coordination spheres of the Sb atoms are completed by additional M atoms and Sb atoms, also, resulting in coordination numbers between 9 and 11. The Sb substructure consists of Sb atoms without Sb−Sb distances < 370 pm as well as a nonlinear Sb_3 unit with interatomic distances of 328 and 344 pm, respectively, while the structure of the binary phosphide Hf_7P_4 exhibits no P−P bonding. The occurrence of Sb−Sb bonds in such a metal-rich antimonide shows a strong tendency of Sb to form homonuclear bonds. Hf_6TiSb_4 is stabilized by M−Sb, M−M, and Sb−Sb bonding interactions, and by a gain in configurational entropy as a consequence of mixed Hf/Ti occupancies.

Acknowledgment. Financial support of the Deutsche Forschungsgemeinschaft, the Fonds der Chemischen Industrie, and the Bundesministerium für Bildung, Wissenschaft, Forschung und Technologie is gratefully acknowledged. Insightful discussions with Professor Dr. B. Harbrecht are appreciated.

Supporting Information Available: One X-ray crystallographic file, in CIF format. This material is available free of charge via the Internet at http://pubs.acs.org.

IC990138M

(29) Weast, R. C. *CRC Handbook of Chemistry and Physics*; CRC Press: Boca Raton, FL 1998.